

1     **The essential genome of *Escherichia coli* K-12**

2

3

4     Emily C. A. Goodall<sup>a</sup>, Ashley Robinson<sup>a</sup>, Iain G. Johnston<sup>a</sup>, Sara Jabbari<sup>a</sup>, Keith A. Turner<sup>b</sup>,

5     Adam. F. Cunningham<sup>a</sup>, Peter A. Lund<sup>a</sup>, Jeffrey A. Cole<sup>a</sup>, Ian R. Henderson<sup>a</sup>#

6

7     Institute of Microbiology and Infection, University of Birmingham, Birmingham, UK<sup>a</sup>;

8     Discuva Ltd, Merrifield Centre, Cambridge, UK<sup>b</sup>,

9

10    Running Head: The essential genome of *E. coli* K-12

11

12    #Address correspondence to Ian R. Henderson, [i.r.henderson@bham.ac.uk](mailto:i.r.henderson@bham.ac.uk)

13    E.C.A.G. and A.R. contributed equally to this work.

14    Abstract word count: 189

15    Text word count: 6,604

## 16 **ABSTRACT**

17 Transposon-Directed Insertion-site Sequencing (TraDIS) is a high-throughput method  
 18 coupling transposon mutagenesis with short-fragment DNA sequencing. It is commonly used  
 19 to identify essential genes. Single gene deletion libraries are considered the gold standard for  
 20 identifying essential genes. Currently, the TraDIS method has not been benchmarked against  
 21 such libraries and therefore it remains unclear whether the two methodologies are  
 22 comparable. To address this, a high density transposon library was constructed in  
 23 *Escherichia coli* K-12. Essential genes predicted from sequencing of this library were  
 24 compared to existing essential gene databases. To decrease false positive identification of  
 25 essential gene candidates, statistical data analysis included corrections for both gene length  
 26 and genome length. Through this analysis new essential genes and genes previously  
 27 incorrectly designated as essential were identified. We show that manual analysis of TraDIS  
 28 data reveals novel features that would not have been detected by statistical analysis alone.  
 29 Examples include short essential regions within genes, orientation-dependent effects and fine  
 30 resolution identification of genome and protein features. Recognition of these insertion  
 31 profiles in transposon mutagenesis datasets will assist genome annotation of less well  
 32 characterized genomes and provides new insights into bacterial physiology and biochemistry.

## 34 **IMPORTANCE**

35 Incentives to define lists of genes that are essential for bacterial survival include the  
 36 identification of potential targets for antibacterial drug development, genes required for rapid  
 37 growth for exploitation in biotechnology, and discovery of new biochemical pathways. To  
 38 identify essential genes in *E. coli*, we constructed a very high density transposon mutant  
 39 library. Initial automated analysis of the resulting data revealed many discrepancies when  
 40 compared to the literature. We now report more extensive statistical analysis supported by

41 both literature searches and detailed inspection of high density TraDIS sequencing data for  
42 each putative essential gene for the model laboratory organism, *Escherichia coli*. This paper  
43 is important because it provides a better understanding of the essential genes of *E. coli*,  
44 reveals the limitations of relying on automated analysis alone and a provides new standard  
45 for the analysis of TraDIS data.

## 46 INTRODUCTION

47 There are many incentives to define lists of genes that are either essential for bacterial  
48 survival or important for normal rates of growth. Essential genes of bacterial pathogens may  
49 encode novel biochemical pathways or potential targets for antibacterial drug development.  
50 Disruption of genes required for rapid growth results in strains handicapped for exploitation  
51 in biotechnology. Conversely, normal growth of mutants defective in genes previously  
52 expected to be essential could reveal unexpected parallel biochemical pathways for fulfilling  
53 the essential function.

54

55 Multiple attempts have been made to generate definitive lists of essential genes, but there are  
56 still many discrepancies between studies even for the model bacterium *Escherichia coli* strain  
57 K-12. Two general approaches have been used: targeted deletion of individual genes, as in  
58 the Keio collection of mutants (1); and random mutagenesis (2, 3). Data from several studies  
59 using different mutagenesis strategies have yielded inconsistent data and hence conflicting  
60 conclusions. Transposon Directed Insertion-site Sequencing (TraDIS) is one of several high-  
61 throughput techniques that combine random transposon mutagenesis with sequencing of the  
62 transposon junctions in high density mutant libraries (4–7). Since its inception in 2009, this  
63 high-throughput method has been applied to a range of biological questions (4, 8–15). Here,  
64 in order to resolve outstanding conflicts, we report the use of this approach to identify the  
65 essential genes of *Escherichia coli* K-12 strain BW25113, a well-studied model organism for  
66 which a complete gene deletion library is available (1).

67

68 A confounding factor in determining the ‘essentiality’ of a gene is the definition of an  
69 essential gene. Complete deletion of an essential gene results, by definition, in a strain that  
70 cannot be isolated following growth. However, it is well known that certain genes are

71 required for growth under specific environmental and nutritional conditions. Such genes can  
72 be considered conditionally essential. For the purposes of this study we define a gene as  
73 essential if the transposon insertion data reveal that the protein coding sequence (CDS), or a  
74 portion of the CDS, is required for growth under the conditions tested here. To aid our  
75 analysis we developed a statistical model that included corrections for both gene length and  
76 genome length in order to decrease false positive identification of essential genes.

77

78 An additional challenge with defining essentiality in high throughput studies is an over-  
79 reliance on automated analysis of the data. For example, a consequence of relying only on  
80 quantification of the number of unique insertions within a gene is that genes with essential  
81 regions will be missed. If only part of a gene encodes the essential function, it should be  
82 possible to isolate viable mutants with transposon insertions in non-essential regions of the  
83 coding sequence (2). Conversely, reliance on statistical analysis alone can also lead to over-  
84 estimation of the number of essential genes. This is a common result from insertion  
85 sequencing analysis (16). A low number of transposon insertion events within a gene, which  
86 fall below the statistical cut-off threshold, can be due to inaccessibility of the gene to  
87 transposition because of extreme DNA structure, exclusion by DNA-binding proteins,  
88 polarity effects due to insertion in a gene upstream of a co-transcribed essential gene, and  
89 location of the gene close to the replication terminus (17). The most frequent reason for a  
90 low number of insertions is that the product of the disrupted gene is required for normal rates  
91 of growth under the conditions tested. In the current study, to minimize the possibility of  
92 incorrectly designating genes as essential or contributing to fitness, we have supported our  
93 statistical analysis with a gene-by-gene inspection of the insertion distribution within each  
94 individual gene.

95

## 96     **RESULTS AND DISCUSSION**

97

### 98     **Sequencing of a mini-Tn5 transposon insertion library in *E. coli* strain BW25113**

99     We have used a modified method to obtain TraDIS data for a transposon mutant library of *E.*  
100     *coli* K-12 strain BW25113 (4, 9). The strain BW25113 was chosen because it is the parent  
101     strain for the Keio collection of deletion mutants and ideal for a direct comparison between  
102     datasets. A mini-Tn5 transposon with a chloramphenicol resistance cassette was transformed  
103     into competent cells and grown overnight on selective medium. Individual colonies were  
104     pooled to construct the initial library, estimated to consist of approximately 3.7 million  
105     mutants. An Illumina MiSeq was used to obtain TraDIS data from two independent DNA  
106     extracts of the transposon library, NTL1 and NTL2 (Table 1). Raw data were checked for the  
107     presence of an inline index barcode to identify independently processed samples (Table 1).  
108     This resulted in 4,818,864 sequence reads from NTL1 and 6,189,409 from NTL2. After  
109     verification of the presence of a transposon sequence and removal of poor quality data or  
110     short sequence reads, 3,891,339 (80.75%) and 4,387,970 (70.89%) sequence reads,  
111     respectively, were mapped successfully to the *E. coli* K-12 BW25113 genome (CP009273.1;  
112     Table 1). The distribution of insertion sites covers the full length of the genome (Fig. 1A).  
113     There was a high correlation coefficient of 0.96 between the samples (Fig. 1B). The data  
114     were therefore combined to give a total of 8,279,317 sequences that were mapped to 901,383  
115     unique insertion sites throughout the genome. Similar numbers of insertions, 481,360 and  
116     480,072, were found for both orientations of the transposon. The high density of unique  
117     insertion sites resulted in an average of 1 insertion every 5.14 bp and a median distance  
118     between insertions of 3 bp. An example is shown in Fig. 1D.

119

### 120     **Identification of putative essential genes by TraDIS**

To determine whether a gene was essential or non-essential the numbers of insertions per CDS were quantified. CDS is defined as the protein coding sequence of a gene, inclusive of the start and stop codons. To normalize for gene length the number of unique insertion points within the CDS was divided by the CDS length in bases. This value was termed the insertion index score and has been used previously as a measure of essentiality (4, 8, 9, 18), given a sufficiently dense library (19).

The frequency distribution of the insertion index scores was bimodal (Fig. S1), as previously shown by others (2). We assume that genes in the left-hand mode, which have a low number of transposon insertions, are either essential for survival or genes that, when disrupted, confer a very severe fitness cost (Fig. 1D). The second mode contains genes with considerably more insertions; these are deemed non-essential (Fig. 1D). Based on inspection of the distributions, an exponential distribution model was fitted to the mode that includes essential genes and a gamma distribution model was fitted to the non-essential mode. For a given insertion index score, the probability of belonging to each mode was calculated and the ratio of these values was termed the log-likelihood score. A gene was classified as essential if its log-likelihood score was less than  $\log_2(12)$  and was therefore 12 times more likely to belong to the essential mode than the non-essential mode. Using this approach, sufficient insertions were found in 3793 genes for them to be classed as non-essential, 162 genes were situated between the two modes and classed as 'unclear' and 358 genes in the mutant library were identified as essential (Table S1).

The 358 candidate essential genes identified in the NTL data were compared to the essential genes as defined by the Keio collection and the Profiling of the *E. coli* Chromosome (PEC) database (1, 2). This comparison revealed 248 genes (59.5%) that were common to all three

datasets (Fig. 2A; Table S2). This agreement between all three datasets strongly supports the hypothesis that these genes are essential so they were not investigated further. An additional 169 genes were identified as potentially essential in only one or two of the datasets. These comprise 16 genes in the Keio and PEC lists that were not identified by our analysis, 25 exclusive to Keio, 18 exclusive to PEC, and 11 and 18 that overlapped between our method and Keio or PEC, respectively (Fig. 2A). However, the largest subcategory of 81 genes is unique to our dataset.

# **Statistical analysis of the transposon insertion density data.**

Over-estimation of the number of genes that are essential has been noted in studies using transposon insertion sequencing (16). In previous attempts to use statistical analysis to define an essential gene, a Poissonian model was used to derive a p-value for an insertion-free region (hereafter IFR) of a given length against the null hypothesis that, by chance, no insertions occurred in that region. We refined this approach for two reasons. First, genomes are sequences of discrete sites: although a continuous Poisson model can provide an approximation to this structure, a naturally discrete picture is more representative of true genome structure. Second, unless corrections are applied for gene length or for the genome length, this method risks overestimating the total number of essential genes. This problem arises because the method implicitly considers only a single, small genomic region, giving the probability that no insertions will be found in a single region of a given bp length. However, genes and genomes have many such regions that are effectively independent, so the genome-wide probability of observing a “false positive” insertion-free region across the genome will be much higher.

170 To avoid this risk of over-interpretation of TraDIS data, we propose a new statistical  
 171 approach, summarized in Supplementary Methods and Supplementary Fig. S2. First, we  
 172 replaced the commonly-used Poissonian model  $\exp(-f/x)$  with a geometric model (see (20)  
 173 for further discussion of this), giving the probability of seeing  $k-1$  "failures" (an insertion-free  
 174 site) then a "success" (insertion event) in a string of independent trials as  $P(k) = p(1-p)^{(k-1)}$ , where  $p$  is the probability of a success (here, an insertion). The  $p$ -value associated with a  
 175 string of  $l$  sites being insertion-free is then  $p = \sum_{k=l}^{\infty} P(k)$ , an easily computable  
 176 quantity. Next, to guard against false positives, we need to precisely state the statistic of  
 177 interest and the corresponding null model. Under a null model of random, independent  
 178 insertions, the three probabilities most pertinent here are those with which (i) a single length- $l$   
 179 region has no insertions; (ii) a gene of length  $g$  contains one or more insertion-free regions of  
 180 length  $l$ ; (iii) a genome of length  $G$  contains one or more insertion-free regions of length  $l$ .  
 181 We used stochastic simulations of random insertions with given densities and genome lengths  
 182 (see Supplementary Methods) to compute these probabilities. These values then give  $p$ -  
 183 values for insertion-free region observations, correcting for gene and genome length.  
 184 Specifically,  $p_{\text{gene}}(l)$  is the probability of observing one or more insertion-free regions of at  
 185 least length  $l$  in a model gene (of length  $g = 1000\text{bp}$ ) by chance (ii), and  $p_{\text{genome}}(l)$  is the  
 186 probability of observing one or more insertion-free regions of at least length  $l$  in a full  
 187 genome (of length  $G = 4.6\text{Mb}$ ) by chance (iii). The uncorrected  $p$ -value (i) is that typically  
 188 reported in other studies. Statistical analysis of our current data (901,383 inserts in a  
 189 4,631,469 bp genome) gives a corrected  $p_{\text{genome}} = 0.05$  for  $l \approx 75$  bp and  $p_{\text{gene}} = 0.05$   
 190 for  $l \approx 36$  bp ( $p_{\text{gene}} = 0.005$  for  $l \approx 47$  bp). In other words, there is a probability of 0.05  
 191 that any insertion-free region of length 75 could appear anywhere in the genome by chance,  
 192 and there is a probability of 0.005 that any insertion-free region of length 47 will occur  
 193 anywhere in a gene of length 1000 by chance. To our knowledge, this represents the first

study with a confident and genome-wide corrected detection resolution (Fig. S2), and the closest yet to approaching the length of the smallest annotated gene in our reference genome (CP009273.1), which is 45 bp.

In checking for uniformity of insertion density across genomic regions, we found that the density of insertions around the terminus (taken as a region centered around *terABCD*) was slightly lower than the genomic average (a density of 0.142 in the surrounding 500 kb region, or 0.145 in the surrounding 1 Mb region, compared to a 0.195 average; Fig. 1A). This density change marginally increases the detection of false-positive essential genes in the vicinity of the terminus, but still represents an unprecedented level of coverage.

## **Resolution of conflicts between datasets**

A critical requirement for the validation of a list of essential genes is to explain why the statistical analysis of transposon insertion data failed to identify genes that the Keio library of deletion mutants and the PEC database identified as essential. We coupled statistical analysis and manual inspection of the data with literature searches to rationalize conflicting results. We find that many of the inconsistencies between datasets can be explained by different methodologies used, definitions of the term ‘essential’ and statistical approaches (Fig. 2B).

**Genes containing transposon free regions.** Manual inspection of the data revealed genes with transposon free regions that were large enough to be identified as significant using the algorithm defined in the previous section. These IFRs do not necessarily report that a gene is essential, but that the insertions within these genes are sufficiently sparse that the IFR is unlikely to have occurred by chance. These genes fall loosely into two groups. The first group contains genes for which the 5’ regions are essential and contain no insertions.

However, there are transposon insertions in the non-essential regions of these genes, such as *ftsK* (Fig. 3A, Table S3). FtsK is involved in correct segregation of the chromosome during division (20, 21); the N-terminal domain of FtsK contains 4 transmembrane passes and is required for localization of FtsK to the septum (22–24). There is substantial literature reporting the essential function of the N-terminal domain, consistent with our data (21, 22, 25). This is a common observation within insertion data and arises when only the function of the N-terminus of the protein is required for viability (8). Initial analysis of transposon insertion data would lead to these genes being incorrectly classified as non-essential, but attempts to construct a deletion mutant would fail. Indeed, previous transposon sequencing experiments failed to identify the essential nature of some of these genes when relying on statistical analysis alone (9).

The second group contains genes with transposon insertion sites throughout the CDS but which have an IFR that passes the significance threshold for essentiality. For example, there is a small IFR within the coding sequence of *secM* of 66 bp (Fig. 3B, Table S3). The *secM* gene is located upstream of the essential gene *secA*. These genes are co-transcribed and also co-translated, and *secM* is known to contain a translational stop sequence that interacts with the ribosomal exit tunnel to halt translation, acting as a translational regulator for *secA*. Specific mutations within the translational stop sequence are lethal unless *secA* is complemented by expression from a plasmid (26). The dependence of *secA* translation on the *secM* CDS would explain the Keio classification as ‘essential’. However, the IFR within *secM* does not fully correspond with the translation stop sequence, suggesting that there is more to be learnt about the translational linkage between the two proteins.

Other researchers have used different approaches to minimize false classification of essential genes during statistical analysis of the insertion profiles by applying a sliding window, quantifying the mean distance between insertions per gene, or variations of truncating the CDS, such as excluding the 3' end, analyzing only the first 60% of the CDS or analyzing the central 60% of the CDS (18, 19, 27–31). However, window analysis may overlook genes such as *secM* and analyzing only the first 60% of the CDS would overlook genes such as *ftsK*.

We suggest that the algorithmic approach used here is a more appropriate method for identifying essential chromosomal regions in a sufficiently dense library. However, we see a number of IFRs >45 bp throughout the genome within non-essential genes, suggesting that our null model of random insertions is not capturing the full structural detail of transposon insertion propensity. This suggests our modelling approach is not based on a perfect representation of biological reality and needs further refinement.

**Polar insertions.** A common feature when creating insertion mutants is the introduction of off-target polar effects where expression of adjacent genes are disrupted by the insertion. To mitigate against such polar effects we designed a cassette that enabled both transcriptional and translational read-through in one direction only. To confirm that transcriptional and translational read-through emanates from the transposon, the transposon was cloned in both orientations and in all three reading frames upstream of the *lacZ* gene in transcription and translation expression vectors pRW224 and pRW225, derivatives of pRW50 (32, 33). Transcriptional read-through was confirmed for one orientation of the transposon, consistent with transcriptional read-through from the chloramphenicol resistance cassette into the downstream disrupted CDS (Fig. 4). Translational read-through was identified for 2 of the 3

open reading frames that coincided with AUG and GUG start codons in the inverted repeat at the end of the transposon. More  $\beta$ -galactosidase activity was obtained from the construct in which the AUG codon was in frame than when the GUG codon that was in frame, confirming that translation was initiated more strongly from the AUG codon. Therefore, transcription is initiated from within the transposon and translation is initiated from within the inverted repeat. This allows transcription and translation of downstream essential regions, even from within a CDS. Such events can be identified by determining to which DNA strand the sequencing data maps (Fig. 4C).

Analysis of our data reveals a number of chromosomal regions with insertions in only one orientation. Such insertion profiles can offer insight into transcriptional regulation of genes when considered in conjunction with neighbouring genes. For example, the gene *rnc* is located in an operon upstream of the essential gene, *era*. Only mutants with transposons that maintain downstream transcription of *era* are viable (Fig. 3C). Baba *et al.* categorized *rnc* as essential (34). However, in the case of the Keio library, construction of an *rnc* deletion mutant would disrupt the ability of the native promoter to drive downstream expression of the essential *era* gene, resulting in apparent lethality. Similarly, in both the Keio and PEC databases *yceQ* is listed as essential but we observed many insertions in *yceQ*, but in only one orientation (Fig. 3D). The gene is located upstream to the essential gene *rne* and is divergently transcribed. The promoter for *rne* is positioned within *yceQ* (35, 36) and deletion of *yceQ* would remove the promoter for *rne* resulting in an apparent lethal effect. Our data reveal that while *era* and *rne* are essential, *rnc* and *yceQ* are not essential.

Like *rnc* and *yceQ*, several of the anti-toxin genes are reported to be essential in the Keio library but not in our dataset or the PEC database (Table S3). Antitoxins are required only if

the corresponding toxin gene is functional. One example is *yefM*. We observed a substantial number of insertions in one orientation. Unlike *rnc* and *yceQ* where insertions maintained downstream expression, in the case of *yefM* the opposite is true; insertions that disrupt expression of the antitoxin but maintain downstream expression of the downstream toxin (*yoeB*) are lethal (Fig. 3E). Scrutiny of our data in this manner reveals these genes are essential.

Another example of insertion bias is observed in a number of genes at the 3' end of a transcript, such as *rplI* (Fig. 3F). While *rplI* is not reported as essential, it is worth noting because insertions restricted exclusively to one orientation within the gene cannot be explained by the positional context between an essential gene and promoter. One possible explanation for this observation is that transcription promoted from the transposon produces an antisense RNA that inhibits expression of an essential gene. Insertion bias, irrespective of the underlying cause, can result in false classification of genes when quantifying insertion index scores as these genes have half as many insertions relative to the rest of the genome. As such, these insertion profiles are to be considered when analyzing data with autonomous statistical approaches.

**Conditionally essential genes.** In addition to the scenarios listed above, certain genes present challenges for binary classification of essentiality. For example, the genes might code for a protein that is essential at a specific phase of growth or for growth under certain environmental parameters such as temperature or nutrient availability. Our data reveal a range of these conditionally essential genes. For instance, the Keio and PEC databases list *folK* as essential whereas we detected multiple insertions within *folK* (Fig. 3G). Loss of *folK* disrupts the ability of the bacterium to produce folate, which is an essential metabolite.

However, supplementation of the medium with folate abrogates the requirement for folate biosynthesis. In addition to *folK*, the Keio and PEC databases report *degS* as essential. In our dataset *degS* has a high density of insertions throughout the CDS suggesting that *degS* is not essential for growth on an agar plate (Fig. 3H). Consistent with this, there is substantial literature showing that *degS* mutants can be isolated, but they either lyse in the stationary phase of growth or rapidly accumulate suppressor mutations (37–40).

The conditional essentiality of such mutants can be tested by growing the transposon library in liquid broth. One would expect mutants lacking *degS* will lyse and that *folK* mutants will be outcompeted as the limited folate available in the medium is depleted. To test these scenarios, two independent samples of the transposon library were grown in LB at 37 °C for 5 to 6 generations to an OD<sub>600</sub> of 1.0 and were then sequenced. These samples, LB1 and LB2, resulted in 5,908,163 and 6,403,324 sequences of which 5,201,711 (88.04%) and 5,382,477 (84.06%), respectively, were mapped to the BW25113 genome (Table 1). Insertion index scores were calculated as before (Table S4). As there was a high correlation coefficient of 0.97 between the gene insertion index scores of each technical replicate (Fig. 1C), the data were combined to give a pool of 10,584,188 sequences. Scrutiny of our data revealed substantially fewer *degS* and *folK* mutants after growth in LB, supporting our hypothesis that they are conditionally essential (Fig. 3G and H). Other genes showing similar fitness costs can be identified in the LB outgrowth dataset (Table S4).

**Errors in library construction.** The difficulty in classifying a gene as essential through deletion analysis is the dependence on a negative result to inform classification. Thus, failure to knock out the gene may result in the false classification of a gene as essential. For example, the Keio database originally reported *mlaB* (*yrbB*) as essential. However, our data

demonstrate that *miaB* is non-essential and this is supported by the literature (41, 42). We have observed similar outcomes for several other genes (Table S3). The reason why knockouts of these genes were not obtained in the construction of the Keio library is unknown.

In addition to the false positive outcomes described above, we noted several instances of false negative results within the Keio library database. For example, both our TraDIS data and the PEC database identified 18 genes as essential that are reported as non-essential in the original Keio database (Table S2). Subsequently, Yamamoto *et al.* (34) demonstrated that for 13 of these mutants the target gene was duplicated during construction of the Keio library resulting in a functional protein; these genes are almost certainly essential. Another difficulty that arises when targeting essential genes for mutagenesis is the potential to select for mutants with a compensatory mutation elsewhere in the genome. Our data revealed *hda* is an essential gene but it is classified as non-essential in the Keio database. Since the initial description of the Keio library, *hda* has been reported to be essential but *hda* mutants rapidly accumulate suppressor mutations that restore viability (43–45). We hypothesise that this is an explanation for the observed essentiality of some genes in the TraDIS dataset that were described as non-essential by others (Table S3). These effects may arise when creating TraDIS libraries but the effects are masked by the large number of mutants in the population.

Similarly, in the PEC library, where insertion density is low, essential genes with an insertion in a non-essential region of the gene will be falsely classified as non-essential when relying on single insertion mutants to inform essentiality. An example of this false negative classification in the PEC database is *tadA* (Table S3). The TadA protein is a tRNA-specific deaminase and its essentiality is reported in the Keio database and our dataset, and is

supported by the literature (46). The PEC database reports a single insertion site within the extreme 3' end of the *tadA* gene.

We have identified a range of underlying causes behind dataset discrepancies and highlight that there are numerous possible insertion profiles for an 'essential' gene. As such, it is important to note that no single statistical method, to our knowledge, would fully identify every essential gene and that manual inspection of data is crucial.

### **Genes identified as essential only by TraDIS.**

There are 81 genes identified as essential using our insertion index data, which are not reported as essential in the Keio or PEC databases (Table 2). These genes fall into two groups, those with no insertions and the remainder with insertions in the CDS. The first group are most likely to be essential. For example, *rpsU* is essential in our data and has been described as essential by others (Fig. 5A; 47). However, in the Keio library there is a duplication event, which gives rise to a mutant that produces a functional protein (34).

Scrutiny of our data for the remaining genes reveals there are additional essential genes with a low frequency of insertions. For instance, *hold* has been described in the literature as an essential gene (48). Our data support that finding (Fig. 5B, Table S1). However, *hold* mutants are available in the Keio collection. The demonstration by Durand *et al.* and others (48–50) that *hold* mutants accumulate extragenic suppressor mutations at high frequency may explain why these mutants are considered non-essential in the Keio database and why we observe a low frequency of insertions in our experiments.

A number of the genes unique to our analysis were not identified as essential in the Keio collection or PEC database simply because they are not included in either of these datasets. This is in part because the Keio collection of knockout mutants was based on available annotation data at the time (51). For example, the identification and location of *ynbG*, *yobI* and *yqcG* was published only in 2008 (52). These genes show very sparse or no transposon disruption in our data and consequently, these genes are potentially essential (Fig. 5C, D and E). Further validation studies would be required to confirm this.

As mentioned previously, over-reporting of essential genes may occur when non-essential genes have low insertion index scores. Such low insertion index scores may arise due to attenuated growth. An example of gene mis-classification because mutation results in a fitness cost and attenuated growth is *guaA*. The low insertion index score results in it being classed as essential despite having many insertions. The fitness effect was confirmed by growing the library in LB, as such mutants are outcompeted (Fig. 5F), and the literature supports the fact that this gene is not essential and has an altered growth rate (53).

### High resolution features within a TraDIS dataset

Manual inspection of a TraDIS dataset can reveal additional information that might go unnoticed in a high throughput analysis pipeline. A common observation from this and previous detailed analysis of data from saturated transposon libraries is the ability to determine, at the bp level of resolution, the boundaries of essential regions within a gene. An example of an essential gene with a dispensable 3' end is *yejM* (*pbgA* in *Salmonella* Typhimurium). Only the 5' end of the CDS is essential, up to and including codon 189, which corresponds with 5 transmembrane helices of the protein structure; the C terminus of the protein is a periplasmic domain that is dispensable for viability (Fig. 6A; 54–56). Our

TraDIS data revealed insertions in codons 186 and 189. Analysis of the transposon orientation at these points revealed that they corresponded with the same transposon insertion location but, due to the 9-bp duplication introduced by the transposon, in different transposon orientations. The introduced transposon sequence maintains codon 189, completely consistent with previously reported results (54, 56).

In addition, as a result of our transposon design, a further feature of our TraDIS data is the identification of genes with dispensable 5' ends. An example of this is *yrfF* which encodes an inhibitor of the Rcs stress response (Fig. 6B; 57, 58). This phenomenon, while less well covered in the literature, is not surprising given that Zhang *et al.* report equal likelihood of a required intragenic region residing at the 5' or 3' end of a gene, albeit in *Mycobacterium tuberculosis* (31). These mutants will only be viable if the remaining CDS can be translated into a functional product and one would expect to find an orientation bias where the transposon drives downstream transcription and translation of the essential region.

Interestingly, inspection of our data revealed essential genes with isolated insertions within the coding sequence. An example of this is *grpE*. The *grpE* gene codes for the essential nucleotide exchange factor that forms a dimer and interacts with DnaK/J complex (59). The insertion occurs only in the orientation that maintains expression of the remaining CDS (Fig. 6C). Mapping of the site of transposon insertion onto the previously determined protein structure of GrpE indicated the insertion occurred within part of the gene encoding a flexible linker between two  $\alpha$ -helices (Fig. 6C). This suggests that a functional GrpE can be expressed as two separate essential domains, and that our TraDIS library has an unprecedented sub-CDS level of resolution to demarcate changes in the protein secondary structure.

443

444 Another fine-resolution mapping feature of our transposon data is the identification of the  
 445 promoter position for essential genes, as also previously reported by Christen *et al.* (8). An  
 446 example of this is the promoter for *lptC*, located within the *kdsD* gene. Three promoters  
 447 (*kdsCp3*, *kdsCp2* and *kdsCp1*) have been identified within the *kdsD* gene (60, 61). However,  
 448 our data show that insertions that maintain expression of *lptC* are tolerated within the *kdsD*  
 449 gene up to *kdsCp2*; insertions stop short just before the *kdsCp2* -35 consensus sequence,  
 450 excluding a single insertion between the -35 and -10, and a single insertion further  
 451 downstream (Fig. 6D). These results suggest that *kdsCp3* is dispensable and at least *kdsCp2*  
 452 is required for adequate expression of *lptC*. As in the case of *grpE* above, this is another  
 453 example of the unprecedented level of genetic detail that can be obtained from this high  
 454 throughput method.

455

456 Finally, within our data we observed a number of transposon-free sections that do not  
 457 correspond with the annotated features of our genome. This can occur when a start codon is  
 458 mis-annotated (8), or translation might initiate at a secondary start codon downstream of the  
 459 transposon insertions. Alternatively, a pseudogene annotation may extend beyond the first  
 460 stop codon. One example of this is *ybbD*, a pseudogene classified as non-essential in our  
 461 dataset. However, the annotation of *ybbD* in the BW25113 genome extends beyond the first  
 462 stop codon, whereas in other genomes it does not, and the region from the methionine  
 463 translation start codon to the first stop codon passes the threshold for essentiality (Fig. 6E).  
 464 In addition, we observed a transposon free region corresponding to *ykiB* (Fig. 6F). This gene  
 465 is annotated in W3110 but not in BW25113, despite the fact the nucleotide sequence is  
 466 identical. Our data suggest that these genes have a significant role in viability or growth but  
 467 further investigation is required to test this. These examples highlight the importance of

having a fully annotated and curated reference genome for mapping data. However, even the highly-studied K-12 genome with its wealth of annotation information retains some as yet unexplained transposon free regions. Thus, TraDIS can help identify regions of genomes where annotation is incorrect or incomplete.

## Conclusion

In summary, the current study has identified 248 genes that are essential for *E. coli* K-12 to survive in standard laboratory conditions (Table S2). We have shown why different conclusions have been drawn from transposon mutagenesis data and gene deletion studies. Essential genes that contain both essential and non-essential regions will statistically appear non-essential if judged only on insertion index scores. We have demonstrated the importance of visual analysis to avoid automation bias in designating genes as essential or non-essential. We have also identified genes incorrectly designated as essential because of failure to recognize polarity effects on a downstream essential gene in the same transcription unit. We also report potential new essential genes and discuss the use of transposon sequencing for fine-resolution mapping of features across the genome. Importantly, TraDIS data are a valuable resource that can be re-inspected following the discovery of new features within a given genome. Finally, our data reveal that there is more to be understood about genome structure and organization, which further coupling of modelling and experimental approaches will help to elucidate.

## MATERIALS AND METHODS

### Strains and plasmids

*E. coli* K-12 strain BW25113, the parent strain of the Keio library, was used for construction of a transposon library. The strain has the following genotype: *rrnB3 ΔlacZ4787 hsdR514*

$\Delta(araBAD)567 \Delta(rhaBAD)568 rph-1$  (62). The transposon mutant library was constructed by collaborators from Discuva, Cambridge, following a method described for *Salmonella* Typhi (4). The main differences were that a mini-Tn5 transposon coding for chloramphenicol resistance cassette resistance was used. This was amplified by PCR from the *cat* gene of the plasmid vector pACYC184 (63) using oligonucleotide primers incorporating the Tn5 transposon mosaic ends. Transposomes were prepared using Tn5 transposase (Epicentre, Madison, WI, USA), and these were introduced into *E. coli* K-12 strain BW25113 by electrotransformation. Transposon mutants were selected by growth on LB agar supplemented with chloramphenicol. Approximately 5.6 million colonies representing an estimated 3.7 million mutants were pooled and stored in 15% glycerol at -80 °C.

## **Media and growth conditions**

DNA was extracted from two samples of the transposon library glycerol stock to generate TraDIS data referred to as NTL1 and NTL2 in the text. In addition, DNA was extracted from two independent cultures, LB1 and LB2, of the library grown in Luria broth (LB: 10 g tryptone, 5 g yeast extract, 10 g NaCl) and grown for 5 to 6 generations at 37 °C with shaking until  $OD_{600} = 1.0$ .

## **Beta-galactosidase assay**

$\beta$ -galactosidase assays were used to measure the activity of transposon::*lacZ* fusions. The transposon was cloned in each orientation, for all three open reading frames, into transcription and translation-assay vectors pRW224 and pRW225 (33). Strains carrying the transposon::*lacZ* fusions were grown overnight at 37 °C with aeration in LB supplemented with 35  $\mu$ g/ml tetracycline (Sigma). The density of the overnight culture was determined by

measuring OD<sub>650</sub> and then used to sub-culture into 5 ml LB and incubated at 37 °C with aeration until the mid-exponential phase of growth (OD<sub>650</sub> of 0.3-0.5). Each culture was lysed by adding 100 µl each of toluene and 1% sodium deoxycholate, mixed by vortex for 15 s and aerating for 20 min at 37 °C. The β-galactosidase activity of each culture was assayed by addition of 100 µl of each culture lysate for three technical replicates to 2.5 ml Z buffer (10 mM KCl, 1 mM MgSO<sub>4</sub>·7H<sub>2</sub>O, 60 mM Na<sub>2</sub>HPO<sub>4</sub>, 30 mM NaH<sub>2</sub>PO<sub>4</sub>·2H<sub>2</sub>O supplemented with 2.7 ml β-mercaptoethanol per litre of distilled water, adjusted to pH 7) supplemented with 13 mM 2-nitrophenyl β-D-galactopyranoside (ONPG; Sigma). The reaction was incubated at 37 °C until a yellow colour had developed, after which the reaction was stopped by adding 1 ml 1 M sodium carbonate. The absorbance of the reaction at OD<sub>420</sub> was measured and β-galactosidase activity was calculated in Miller units.

### **TraDIS Sequencing**

Harvested cells were prepared for sequencing following an amended TraDIS protocol (4, 8, 9). Genomic DNA was isolated using a Qiagen QIAamp DNA Blood Mini Kit, according to the manufacturer's specifications. DNA was quantified and mechanically sheared by ultrasonication. Sheared DNA fragments were processed for sequencing using NEB Next Ultra I kit. Following adaptor ligation, a PCR step was introduced to enrich for transposon-containing fragments, using a forward primer specific for the transposon 3' end and a reverse primer specific for the adapter. After PCR-purification, an additional PCR prepared DNA for sequencing through the addition of Illumina-specific flow cell adaptor sequences and custom inline index barcodes of variable length in the forward primers. The purpose of this was to increase indexing capacity while staggering introduction of the transposon sequence to increase base diversity during sequencing. Samples were sequenced using Illumina MiSeq 150 cycle v3 cartridges, aiming for an optimal cluster density of 800 clusters per mm<sup>2</sup>.

543

## 544 **Sequencing analysis**

545 Raw data was collected and analyzed using a series of custom scripts. The Fastx barcode  
546 splitter and trimmer tools, of the Fastx toolkit, were used to assess and trim the sequences  
547 (64). Sequence reads were first filtered by their inline indexes, allowing no mismatches.  
548 Transposon similarity matching was done by identifying the first 35 bp of the transposon 5'  
549 end in two parts: 25 bases (5' to 3') were matched allowing for 3 mismatches, trimmed, and  
550 then the remaining 10 bases matched allowing for 1 mismatch, and trimmed. Sequences less  
551 than 20 bases long were removed using Trimmomatic (65). Trimmed, filtered sequences  
552 were then aligned to the reference genome *E. coli* BW25113 (CP009273.1), obtained from  
553 the NCBI genome repository (66). Where gene names differed between databases, the  
554 BW25113 annotation was used. The aligner bwa was used, with the mem algorithm (0.7.8-  
555 r455; 55). Aligned reads were filtered to remove any soft clipped reads. The subsequent  
556 steps of conversion from sam files to bam files, and the requisite sorting and indexing, were  
557 done using samtools (0.1.19-44428cd; 68). The bedtools suite was used to create bed files  
558 which were intersected against the coding sequence boundaries defined in general feature  
559 format (.gff) files obtained from NCBI (69). Custom python scripts were used to quantify  
560 insertion sites within the annotated CDS boundaries. Data were inspected manually using the  
561 Artemis genome browser (70).

562

## 563 **Essential gene prediction**

564 The frequency of insertion indices was plotted in a histogram using the Freedman–Diaconis  
565 rule for choice of bin-widths (Figure S1). Using the R MASS library ([http://www.r-](http://www.r-project.org)  
566 [project.org](http://www.r-project.org)), an exponential distribution (red line) was fitted to the left, “essential” mode (i.e.  
567 any data to the left of the trough in Figure S1); a gamma distribution (blue line) was fitted to

the right, “non-essential” mode (i.e. any data to the right of the trough). The probability of a gene belonging to each mode was calculated and the ratio of these values was used to calculate a log-likelihood score. Using a 12-fold likelihood threshold, based on the log-likelihood scores, genes were assigned as “essential” if they were 12 times more likely to be in the left mode than the right mode, and “non-essential” if they were 12-times more likely to be in the right mode (9). Genes with log-likelihood scores between the upper and lower  $\log_2(12)$  threshold values of 3.6 and -3.6 respectively were deemed “unclear”. A threshold cut-off of  $\log_2(12)$  was chosen as it is more stringent than  $\log_2(4)$  (used by Langridge *et al.*; 4), and consistent with analysis used by Phan *et al.* (9).

## Essential gene lists

The Keio essential gene list is composed of the original essential genes minus three ORFs, JW5190, JW5193 and JW5379, as they are not annotated within MG1655 and are thought to be spurious, giving a final list of 300 genes (1, 71). The PEC dataset is composed of the 300 genes listed as essential for W3110 (2). The lists of essential genes were compared using BioVenn (72).

## Statistical Analysis

For details of the statistical analysis, see Supplementary materials and methods and Figures S1 and S2.

## FUNDING INFORMATION

This research has been supported by the Midlands Integrative Biosciences Training Partnership (MIBTP, BBSRC) PhD programme, and the University of Birmingham Elite PhD

592 Scholarship to IRH. IGJ is supported by a Birmingham Fellowship. SJ is supported by the  
593 BBSRC and MRC.

594

## 595 **ACKNOWLEDGEMENTS**

596 We thank Discuva Ltd. for providing some of their large transposon mutant library. We  
597 thank N. Loman and J. Quick for help with optimization of our MiSeq protocol. We thank  
598 the authors of Langridge *et al.* (2009) for kindly supplying their R code for essential gene  
599 prediction. We thank Tony Hitchcock and Steve Williams for their support, and Cobrabio for  
600 their contribution to the University of Birmingham Elite PhD studentship. Lastly, we thank  
601 M.J. Collingwood and R.W. Meek for their generous help with drawing figures.

## REFERENCES

1. Baba T, Ara T, Hasegawa M, Takai Y, Okumura Y, Baba M, Datsenko K a, Tomita M, Wanner BL, Mori H. 2006. Construction of Escherichia coli K-12 in-frame, single-gene knockout mutants: the Keio collection. *Mol Syst Biol* 2:2006.0008.
2. Yamazaki Y, Niki H, Kato J. 2008. Profiling of Escherichia coli Chromosome database. *Methods Mol Biol* 416:385–9.
3. Nguyen BD, Valdivia RH. 2012. Virulence determinants in the obligate intracellular pathogen Chlamydia trachomatis revealed by forward genetic approaches. *Proc Natl Acad Sci U S A* 109:1263–8.
4. Langridge GC, Phan MD, Turner DJ, Perkins TT, Parts L, Haase J, Charles I, Maskell DJ, Peters SE, Dougan G, Wain J, Parkhill J, Turner a. K. 2009. Simultaneous assay of every Salmonella Typhi gene using one million transposon mutants. *Genome Res* 19:2308–2316.
5. van Opijnen T, Bodi KL, Camilli A. 2009. Tn-seq: high-throughput parallel sequencing for fitness and genetic interaction studies in microorganisms. *Nat Methods* 6:767–72.
6. Gawronski JD, Wong SMS, Giannoukos G, Ward D V, Akerley BJ. 2009. Tracking insertion mutants within libraries by deep sequencing and a genome-wide screen for Haemophilus genes required in the lung. *Proc Natl Acad Sci U S A* 106:16422–7.
7. Goodman AL, McNulty NP, Zhao Y, Leip D, Mitra RD, Lozupone CA, Knight R, Gordon JI. 2009. Identifying genetic determinants needed to establish a human gut symbiont in its habitat. *Cell Host Microbe* 6:279–89.
8. Christen B, Abeliuk E, Collier JM, Kalogeraki VS, Passarelli B, Collier JA, Fero MJ, McAdams HH, Shapiro L. 2014. The essential genome of a bacterium. *Mol Syst Biol* 7:528–528.

- 627 9. Phan MD, Peters KM, Sarkar S, Lukowski SW, Allsopp LP, Moriel DG, Achard MES,  
628 Totsika M, Marshall VM, Upton M, Beatson S a., Schembri M a. 2013. The serum  
629 resistome of a globally disseminated multidrug resistant uropathogenic *Escherichia*  
630 *coli* clone. *PLoS Genet* 9.
- 631 10. Hassan KA, Cain AK, Huang T, Liu Q, Elbourne LDH, Boinett CJ, Brzoska AJ, Li L,  
632 Ostrowski M, Nhu NTK, Nhu TDH, Baker S, Parkhill J, Paulsen IT. 2016.  
633 Fluorescence-Based Flow Sorting in Parallel with Transposon Insertion Site  
634 Sequencing Identifies Multidrug Efflux Systems in *Acinetobacter baumannii*. *MBio*  
635 7:e01200-16.
- 636 11. Paulsen IT, Cain AK, Hassan KA. 2017. Physical enrichment of transposon mutants  
637 from saturation mutant libraries using the TraDISort approach. *Mob Genet Elements*  
638 7:1–7.
- 639 12. Parsons AB, Brost RL, Ding H, Li Z, Zhang C, Sheikh B, Brown GW, Kane PM,  
640 Hughes TR, Boone C. 2004. Integration of chemical-genetic and genetic interaction  
641 data links bioactive compounds to cellular target pathways. *Nat Biotechnol* 22:62–9.
- 642 13. Grant AJ, Oshota O, Chaudhuri RR, Mayho M, Peters SE, Clare S, Maskell DJ,  
643 Mastroeni P. 2016. Genes Required for the Fitness of *Salmonella enterica* Serovar  
644 Typhimurium during Infection of Immunodeficient *gp91<sup>-/-</sup> phox* Mice. *Infect Immun*  
645 84:989–997.
- 646 14. Troy EB, Lin T, Gao L, Lazinski DW, Lundt M, Camilli A, Norris SJ, Hu LT. 2016.  
647 Global Tn-seq analysis of carbohydrate utilization and vertebrate infectivity of  
648 *Borrelia burgdorferi*. *Mol Microbiol* 101:1003–1023.
- 649 15. Mann B, van Opijnen T, Wang J, Obert C, Wang Y-D, Carter R, McGoldrick DJ,  
650 Ridout G, Camilli A, Tuomanen EI, Rosch JW. 2012. Control of virulence by small  
651 RNAs in *Streptococcus pneumoniae*. *PLoS Pathog* 8:e1002788.

- 652 16. Grenov AI, Gerdes SY. 2008. Modeling competitive outgrowth of mutant populations:  
653 why do essentiality screens yield divergent results?, p. 361–367. *In* Methods in  
654 molecular biology (Clifton, N.J.).
- 655 17. Manna D, Porwollik S, McClelland M, Tan R, Higgins NP. 2007. Microarray analysis  
656 of Mu transposition in *Salmonella enterica*, serovar Typhimurium: transposon  
657 exclusion by high-density DNA binding proteins. *Mol Microbiol* 66:315–28.
- 658 18. Curtis PD, Brun Y V. 2014. Identification of essential alphaproteobacterial genes  
659 reveals operational variability in conserved developmental and cell cycle systems. *Mol*  
660 *Microbiol* 93:713–35.
- 661 19. Solaimanpour S, Sarmiento F, Mrázek J. 2015. Tn-seq explorer: a tool for analysis of  
662 high-throughput sequencing data of transposon mutant libraries. *PLoS One*  
663 10:e0126070.
- 664 20. Liu G, Draper GC, Donachie WD. 1998. FtsK is a bifunctional protein involved in cell  
665 division and chromosome localization in *Escherichia coli*. *Mol Microbiol* 29:893–903.
- 666 21. Dubarry N, Possoz C, Barre F-X. 2010. Multiple regions along the *Escherichia coli*  
667 FtsK protein are implicated in cell division. *Mol Microbiol* 78:1088–1100.
- 668 22. Draper GC, McLennan N, Begg K, Masters M, Donachie WD. 1998. Only the N-  
669 terminal domain of FtsK functions in cell division. *J Bacteriol* 180:4621–7.
- 670 23. Yu XC, Tran AH, Sun Q, Margolin W. 1998. Localization of cell division protein FtsK  
671 to the *Escherichia coli* septum and identification of a potential N-terminal targeting  
672 domain. *J Bacteriol* 180:1296–304.
- 673 24. Dorazi R, Dewar SJ. 2000. Membrane topology of the N-terminus of the *Escherichia*  
674 *coli* FtsK division protein. *FEBS Lett* 478:13–8.
- 675 25. Wang L, Lutkenhaus J. 1998. FtsK is an essential cell division protein that is localized  
676 to the septum and induced as part of the SOS response. *Mol Microbiol* 29:731–40.

- 677 26. Murakami A, Nakatogawa H, Ito K. 2004. Translation arrest of SecM is essential for  
678 the basal and regulated expression of SecA. *Proc Natl Acad Sci U S A* 101:12330–5.
- 679 27. DeJesus MA, Ioerger TR. 2013. A Hidden Markov Model for identifying essential and  
680 growth-defect regions in bacterial genomes from transposon insertion sequencing data.  
681 *BMC Bioinformatics* 14:303.
- 682 28. Freed NE, Bumann D, Silander OK. 2016. Combining *Shigella* Tn-seq data with gold-  
683 standard *E. coli* gene deletion data suggests rare transitions between essential and non-  
684 essential gene functionality. *BMC Microbiol* 16:203.
- 685 29. Zomer A, Burghout P, Bootsma HJ, Hermans PWM, van Hijum SAFT. 2012.  
686 ESSENTIALS: software for rapid analysis of high throughput transposon insertion  
687 sequencing data. *PLoS One* 7:e43012.
- 688 30. Sarmiento F, Mrázek J, Whitman WB. 2013. Genome-scale analysis of gene function  
689 in the hydrogenotrophic methanogenic archaeon *Methanococcus maripaludis*. *Proc*  
690 *Natl Acad Sci U S A* 110:4726–31.
- 691 31. Zhang YJ, Ioerger TR, Huttenhower C, Long JE, Sasseti CM, Sacchettini JC, Rubin  
692 EJ. 2012. Global assessment of genomic regions required for growth in  
693 *Mycobacterium tuberculosis*. *PLoS Pathog* 8:e1002946.
- 694 32. Lodge J, Fear J, Busby S, Gunasekaran P, Kamini NR. 1992. Broad host range  
695 plasmids carrying the *Escherichia coli* lactose and galactose operons. *FEMS Microbiol*  
696 *Lett* 95:271–276.
- 697 33. Islam MS, Shaw RK, Frankel G, Pallen MJ, Busby SJW. 2012. Translation of a  
698 minigene in the 5' leader sequence of the enterohaemorrhagic *Escherichia coli* LEE1  
699 transcription unit affects expression of the neighbouring downstream gene. *Biochem J*  
700 441:247–53.
- 701 34. Yamamoto N, Nakahigashi K, Nakamichi T, Yoshino M, Takai Y, Touda Y,

- 702 Furubayashi A, Kinjyo S, Dose H, Hasegawa M, Datsenko KA, Nakayashiki T,  
703 Tomita M, Wanner BL, Mori H. 2009. Update on the Keio collection of *Escherichia*  
704 *coli* single-gene deletion mutants. *Mol Syst Biol* 5:335.
- 705 35. Claverie-Martin F, Diaz-Torres MR, Yancey SD, Kushner SR. 1991. Analysis of the  
706 altered mRNA stability (*ams*) gene from *Escherichia coli*. Nucleotide sequence,  
707 transcriptional analysis, and homology of its product to MRP3, a mitochondrial  
708 ribosomal protein from *Neurospora crassa*. *J Biol Chem* 266:2843–51.
- 709 36. Ow MC, Liu Q, Mohanty BK, Andrew ME, Maples VF, Kushner SR. 2002. RNase E  
710 levels in *Escherichia coli* are controlled by a complex regulatory system that involves  
711 transcription of the *rne* gene from three promoters. *Mol Microbiol* 43:159–71.
- 712 37. Ades SE, Connolly LE, Alba BM, Gross CA. 1999. The *Escherichia coli* sigma(E)-  
713 dependent extracytoplasmic stress response is controlled by the regulated proteolysis  
714 of an anti-sigma factor. *Genes Dev* 13:2449–61.
- 715 38. Alba BM, Zhong HJ, Pelayo JC, Gross CA. 2001. *degS* (*hhoB*) is an essential  
716 *Escherichia coli* gene whose indispensable function is to provide sigma (E) activity.  
717 *Mol Microbiol* 40:1323–33.
- 718 39. Bass S, Gu Q, Christen A. 1996. Multicopy suppressors of *prc* mutant *Escherichia coli*  
719 include two HtrA (DegP) protease homologs (HhoAB), DksA, and a truncated R1pA. *J*  
720 *Bacteriol* 178:1154–61.
- 721 40. Waller PR, Sauer RT. 1996. Characterization of *degQ* and *degS*, *Escherichia coli*  
722 genes encoding homologs of the DegP protease. *J Bacteriol* 178:1146–53.
- 723 41. Malinverni JC, Silhavy TJ. 2009. An ABC transport system that maintains lipid  
724 asymmetry in the Gram-negative outer membrane. *Proc Natl Acad Sci* 106:8009–  
725 8014.
- 726 42. Thong S, Ercan B, Torta F, Fong ZY, Wong HYA, Wenk MR, Chng S-S. 2016.

- 727 Defining key roles for auxiliary proteins in an ABC transporter that maintains bacterial  
728 outer membrane lipid asymmetry. *Elife* 5.
- 729 43. Kato J, Katayama T. 2001. Hda, a novel DnaA-related protein, regulates the  
730 replication cycle in *Escherichia coli*. *EMBO J* 20:4253–4262.
- 731 44. Riber L, Olsson JA, Jensen RB, Skovgaard O, Dasgupta S, Marinus MG, Løbner-  
732 Olesen A. 2006. Hda-mediated inactivation of the DnaA protein and dnaA gene  
733 autoregulation act in concert to ensure homeostatic maintenance of the *Escherichia coli*  
734 chromosome. *Genes Dev* 20:2121–2134.
- 735 45. Camara JE, Skarstad K, Crooke E. 2003. Controlled initiation of chromosomal  
736 replication in *Escherichia coli* requires functional Hda protein. *J Bacteriol* 185:3244–8.
- 737 46. Wolf J, Gerber AP, Keller W. 2002. tadA, an essential tRNA-specific adenosine  
738 deaminase from *Escherichia coli*. *EMBO J* 21:3841–51.
- 739 47. Bubunenko M, Baker T, Court DL. 2007. Essentiality of ribosomal and transcription  
740 antitermination proteins analyzed by systematic gene replacement in *Escherichia coli*.  
741 *J Bacteriol* 189:2844–2853.
- 742 48. Durand A, Sinha AK, Dard-Dascot C, Michel B. 2016. Mutations Affecting Potassium  
743 Import Restore the Viability of the *Escherichia coli* DNA Polymerase III holD Mutant.  
744 *PLOS Genet* 12:e1006114.
- 745 49. Viguera E, Petranovic M, Zahradka D, Germain K, Ehrlich DS, Michel B. 2003.  
746 Lethality of bypass polymerases in *Escherichia coli* cells with a defective clamp loader  
747 complex of DNA polymerase III. *Mol Microbiol* 50:193–204.
- 748 50. Duigou S, Silvain M, Viguera E, Michel B. 2014. ssb Gene Duplication Restores the  
749 Viability of  $\Delta$ holC and  $\Delta$ holD *Escherichia coli* Mutants. *PLoS Genet* 10:e1004719.
- 750 51. Riley M, Abe T, Arnaud MB, Berlyn MKB, Blattner FR, Chaudhuri RR, Glasner JD,  
751 Horiuchi T, Keseler IM, Kosuge T, Mori H, Perna NT, Plunkett G, Rudd KE, Serres

752 MH, Thomas GH, Thomson NR, Wishart D, Wanner BL. 2006. Escherichia coli K-12:  
753 a cooperatively developed annotation snapshot--2005. Nucleic Acids Res 34:1–9.

754 52. Hemm MR, Paul BJ, Schneider TD, Storz G, Rudd KE. 2008. Small membrane  
755 proteins found by comparative genomics and ribosome binding site models. Mol  
756 Microbiol 70:1487–501.

757 53. Davies IJ, Drabble WT. 1996. Stringent and growth-rate-dependent control of the gua  
758 operon of Escherichia coli K-12. Microbiology 142:2429–2437.

759 54. De Lay NR, Cronan JE. 2008. Genetic interaction between the Escherichia coli AcpT  
760 phosphopantetheinyl transferase and the YejM inner membrane protein. Genetics  
761 178:1327–37.

762 55. Daley DO, Rapp M, Granseth E, Melén K, Drew D, von Heijne G. 2005. Global  
763 topology analysis of the Escherichia coli inner membrane proteome. Science (80- )  
764 308:1321–1323.

765 56. Dalebroux ZD, Edrozo MB, Pfuetschner RA, Ressler S, Kulasekara BR, Blanc M-P, Miller  
766 SI. 2015. Delivery of cardiolipins to the Salmonella outer membrane is necessary for  
767 survival within host tissues and virulence. Cell Host Microbe 17:441–51.

768 57. Cano DA, Domínguez-Bernal G, Tierrez A, Garcia-Del Portillo F, Casadesús J. 2002.  
769 Regulation of capsule synthesis and cell motility in Salmonella enterica by the  
770 essential gene igaA. Genetics 162:1513–23.

771 58. Cho S-H, Szewczyk J, Pesavento C, Zietek M, Banzhaf M, Roszczenko P, Asmar A,  
772 Laloux G, Hov A-K, Leverrier P, Van der Henst C, Vertommen D, Typas A, Collet J-  
773 F. 2014. Detecting Envelope Stress by Monitoring  $\beta$ -Barrel Assembly. Cell 159:1652–  
774 1664.

775 59. Harrison CJ, Hayer-Hartl M, Di Liberto M, Hartl F, Kuriyan J. 1997. Crystal structure  
776 of the nucleotide exchange factor GrpE bound to the ATPase domain of the molecular

777        chaperone DnaK. *Science* 276:431–5.

778    60.    Martorana AM, Sperandeo P, Polissi A, Dehò G. 2011. Complex transcriptional  
779        organization regulates an *Escherichia coli* locus implicated in lipopolysaccharide  
780        biogenesis. *Res Microbiol* 162:470–482.

781    61.    Sperandeo P, Pozzi C, Dehò G, Polissi A. 2006. Non-essential KDO biosynthesis and  
782        new essential cell envelope biogenesis genes in the *Escherichia coli* yrbG–yhbG locus.  
783        *Res Microbiol* 157:547–558.

784    62.    Datsenko KA, Wanner BL. 2000. One-step inactivation of chromosomal genes in  
785        *Escherichia coli* K-12 using PCR products. *Proc Natl Acad Sci U S A* 97:6640–5.

786    63.    Chang AC, Cohen SN. 1978. Construction and characterization of amplifiable  
787        multicopy DNA cloning vehicles derived from the P15A cryptic miniplasmid. *J*  
788        *Bacteriol* 134:1141–56.

789    64.    Pearson WR, Wood T, Zhang Z, Miller W. 1997. Comparison of DNA Sequences with  
790        Protein Sequences. *Genomics* 46:24–36.

791    65.    Bolger AM, Lohse M, Usadel B. 2014. Trimmomatic: a flexible trimmer for Illumina  
792        sequence data. *Bioinformatics* 30:2114–2120.

793    66.    Tatusova T, Ciufo S, Fedorov B, O’Neill K, Tolstoy I. 2014. RefSeq microbial  
794        genomes database: new representation and annotation strategy. *Nucleic Acids Res*  
795        42:D553-9.

796    67.    Li H, Durbin R. 2009. Fast and accurate short read alignment with Burrows-Wheeler  
797        transform. *Bioinformatics* 25:1754–1760.

798    68.    Li H, Handsaker B, Wysoker A, Fennell T, Ruan J, Homer N, Marth G, Abecasis G,  
799        Durbin R, 1000 Genome Project Data Processing Subgroup. 2009. The Sequence  
800        Alignment/Map format and SAMtools. *Bioinformatics* 25:2078–2079.

801    69.    Quinlan AR, Hall IM. 2010. BEDTools: a flexible suite of utilities for comparing

802 genomic features. *Bioinformatics* 26:841–842.

803 70. Rutherford K, Parkhill J, Crook J, Horsnell T, Rice P, Rajandream MA, Barrell B.

804 2000. Artemis: sequence visualization and annotation. *Bioinformatics* 16:944–5.

805 71. Zhou J, Rudd KE. 2013. EcoGene 3.0. *Nucleic Acids Res* 41:D613-24.

806 72. Hulsen T, de Vlieg J, Alkema W. 2008. BioVenn - a web application for the

807 comparison and visualization of biological lists using area-proportional Venn

808 diagrams. *BMC Genomics* 9:488.

809

810 Table 1. Parameters for TraDIS data set derived from the *E. coli* K-12 strain BW25113  
811 transposon library  
812

Condition	Number of sequence reads with matching inline barcode	Mapped sequence reads	Number of genome-wide insertion sites
NTL1	4,818,864	3,891,339 (80.75% of the raw data)	500,476
NTL2	6,189,409	4,387,970 (70.89% of the raw data)	817,011
NTL combined	11,008,273	8,279,309	901,383
LB1	5,908,163	5,201,711 (88.04% of the raw data)	400,009
LB2	6,403,324	5,382,477 (84.06% of the raw data)	419,660
LB combined	12,311,487	10,584,188	595,233

813

814 Table 2. Genes with low insertion index scores identified by TraDIS only  
815

Gene	Function	Comments
<b>Genes with no insertions</b>		
<i>glyA</i>	Serine hydroxymethyltransferase	
<i>pheM</i>	<i>pheST</i> operon leader peptide	
<i>rimM</i>	Ribosome maturation protein	
<i>rplK</i>	50S ribosomal subunit	Duplicated in Keio collection <sup>a</sup>
<i>rplY</i>	50S ribosomal subunit	Duplicated in Keio collection
<i>rpmF</i>	50S ribosomal subunit	
<i>rpmI</i>	50S ribosomal subunit	
<i>rpsF</i>	30S ribosomal subunit	
<i>rpsO</i>	30S ribosomal subunit	Duplicated in Keio collection
<i>rpsT</i>	30S ribosomal subunit	
<i>rpsU</i>	30S ribosomal subunit	Duplicated in Keio collection
<i>thyA</i>	Thymidylate synthase	
<i>ttcC</i>	Pseudogene	
<i>ynbG</i>	Small protein	
<b>Genes with a low frequency of insertions</b>		
<i>aceF</i>	Pyruvate dehydrogenase, E2 subunit	
<i>cydB</i>	Cytochrome bd-I terminal oxidase subunit II	
<i>cydD</i>	Glutathione/L-cysteine exporter	
<i>cydX</i>	Cytochrome bd-I terminal oxidase	
<i>dapF</i>	Diaminopimelate epimerase	
<i>dcd</i>	dCTP deaminase	
<i>fabH</i>	$\beta$ -ketoacyl-ACP synthase III	
<i>fdx</i>	Reduced ferredoxin	
<i>folP</i>	Dihydropteroate synthase	Duplicated in Keio collection
<i>guaA</i>	GMP synthetase	
<i>hemE</i>	Uroporphyrinogen decarboxylase	Duplicated in Keio collection
<i>higA</i>	Antitoxin of the HigB-HigA toxin-antitoxin system	
<i>hipB</i>	HipB antitoxin and DNA-binding transcriptional repressor	
<i>holD</i>	DNA polymerase III, $\Psi$ subunit	
<i>hscA</i>	Chaperone for [Fe-S] cluster biosynthesis	
<i>ihfA</i>	Integration host factor (IHF), $\alpha$ subunit	
<i>iraM</i>	Anti-adaptor protein iraM, inhibitor of $\sigma$ S proteolysis	
<i>iscS</i>	Cysteine desulfurase	
<i>iscU</i>	Scaffold protein for iron-sulfur cluster assembly	
<i>lipA</i>	Lipoyl synthase	
<i>lpd</i>	Lipoamide dehydrogenase	
<i>lpxL</i>	Lauroyl acyltransferase	
<i>lysS</i>	Lysine-tRNA ligase	

<i>mmmA</i>	tRNA-specific 2-thiouridylase	
<i>pdxH</i>	pyridoxine 5'-phosphate oxidase / pyridoxamine 5'-phosphate oxidase	
<i>priB</i>	Primosomal replication protein N	Duplicated in Keio collection.
<i>ptsI</i>	PTS enzyme I	
<i>rbfA</i>	30S ribosome binding factor	
<i>relB</i>	RelB-antitoxin and DNA-binding transcriptional repressor	
<i>rluD</i>	23S rRNA pseudouridine synthase	
<i>rnt</i>	RNase T	
<i>rpe</i>	Ribulose-5-phosphate 3-epimerase	
<i>rplA</i>	50S ribosomal subunit	
<i>safA</i>	EvgS/EvgA and PhoQ/PhoP connector	
<i>sucA</i>	2-oxoglutarate decarboxylase	
<i>sucB</i>	Dihydrolipoyltranssuccinylase	
<i>tktA</i>	Transketolase I	
<i>tonB</i>	TonB energy transducing system - TonB subunit	
<i>trpL</i>	<i>trp</i> operon leader peptide	
<i>tusE</i>	Sulfur transfer protein	
<i>ubiE</i>	Bifunctional 2-octaprenyl-6-methoxy-1,4-benzoquinone methylase and S-adenosylmethionine:2-DMK methyltransferase	
<i>ubiG</i>	Bifunctional 3-demethylubiquinone-8 3-O-Methyltransferase and 2-octaprenyl-6-hydroxyphenol methylase	
<i>ubiH</i>	2-octaprenyl-6-methoxyphenol hydroxylase	
<i>ubiX</i>	3-octaprenyl-4-hydroxybenzoate carboxy-lyase partner protein	
<i>ybeY</i>	Endoribonuclease involved in maturation of 16S rRNA and ribosome quality control	
<i>ycaR</i>	Conserved protein	
<i>yciS</i>	Lipopolysaccharide assembly protein	
<i>ydaE</i>	Rac prophage; zinc-binding protein	
<i>ydaS</i>	Rac prophage; predicted DNA-binding transcriptional regulator	
<i>ycdD</i>	Hypothetical protein	
<i>yddL</i>	Predicted lipoprotein	
<i>ydfO</i>	Qin prophage; predicted protein	
<i>ydhL</i>	Conserved protein	
<i>yedN</i>	Putative protein	
<i>yffS</i>	CPZ-55 prophage	
<i>ygeF</i>	Predicted protein	
<i>ygeG</i>	Predicted chaperone	
<i>ygeN</i>	Predicted protein	
<i>ygfZ</i>	Folate-binding protein	
<i>yjbS</i>	Hypothetical protein	
<i>ykfM</i>	Hypothetical protein	
<i>ymfE</i>	e14 prophage; predicted inner membrane protein	
<i>ymiB</i>	Putative protein	
<i>yncH</i>	Hypothetical protein	

<i>yobI</i>	Small protein
<i>yqcG</i>	Cell envelope stress response protein
<i>yqeL</i>	Small protein

---

816

817 <sup>a</sup>Yamamoto *et al.* 2009

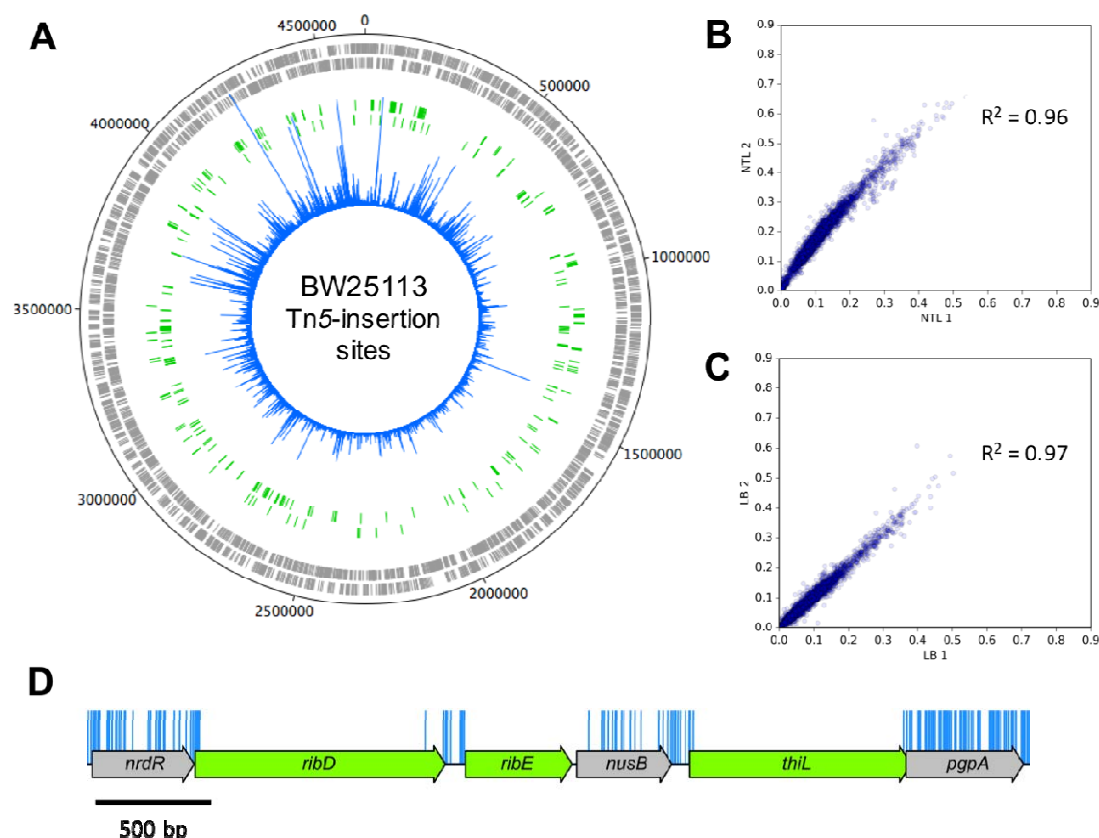


**Figure 1. Genome wide transposon insertion sites mapped to *E. coli* strain BW25113.**

(A) Frequency and location of transposon junction sequences from a mini-Tn5 transposon library in strain BW25113, mapped to the BW25113 genome (CP009273.1). The outer track marks the BW25113 genome in bp starting at the annotation origin. The next two inner tracks correspond to sense and anti-sense CDS respectively (grey), followed by two inner tracks depicting the essential genes identified by TraDIS on the sense and anti-sense strands, respectively (green). The innermost circle (blue) corresponds to the frequency and location of transposon insertion sequences mapped successfully to the BW25113 genome after identification of a transposon sequence. Figure created using DNAPlotter. (B) The correlation coefficient of gene insertion index scores for two sequenced technical replicates of the input transposon library (NTL1 and NTL2) (C) and following growth in LB (LB1 and LB2). (D) Representation of transposon insertion points across a portion of the K-12 BW25113 genome (blue), showing essential genes (green) and non-essential genes (grey).

832 Blue bars correspond with transposon insertion sites along the genome and have been capped  
833 at a frequency of 1.

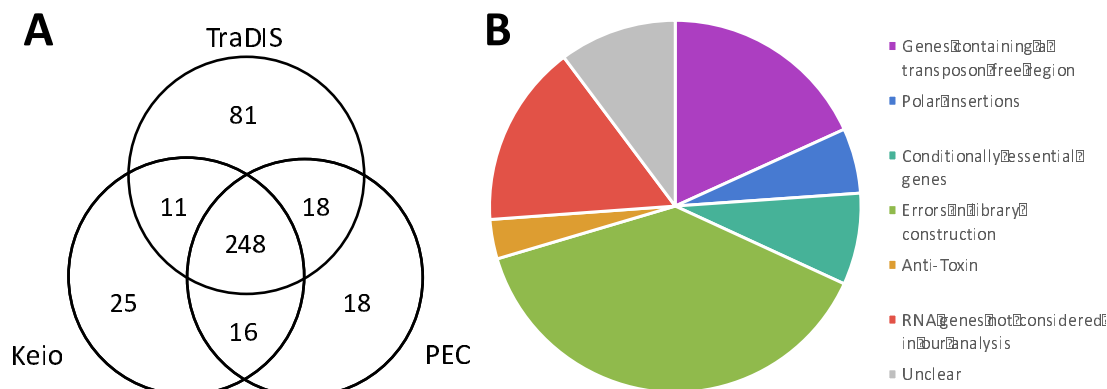


**Figure 2. Comparison of essential gene data from various sources and examples of insertion profiles overlooked by automated statistical analysis of insertion index scores.**

(A) Essential gene candidates identified using TraDIS were compared to existing essential gene data. A 3-way comparison between the Keio collection of single gene knockouts, the Profiling of the *E. coli* Chromosome (PEC) online database and our transposon-insertion sequencing data identified 248 essential genes that were common to all three data. (B) The outlying genes of the Venn diagram, excluding those unique to our TraDIS dataset, were inspected to understand the source of discrepancy between datasets. Genes were grouped into the overarching categories of “Transposon free region” (blue), “Anti-toxin” (green), “Polar insertions” (purple), “Conditionally essential” (orange), and “Errors in library construction” (red) with subcategories depicted in different shades of the colour. Genes not included in our analysis or that remain unclear are shown in yellow or grey respectively.

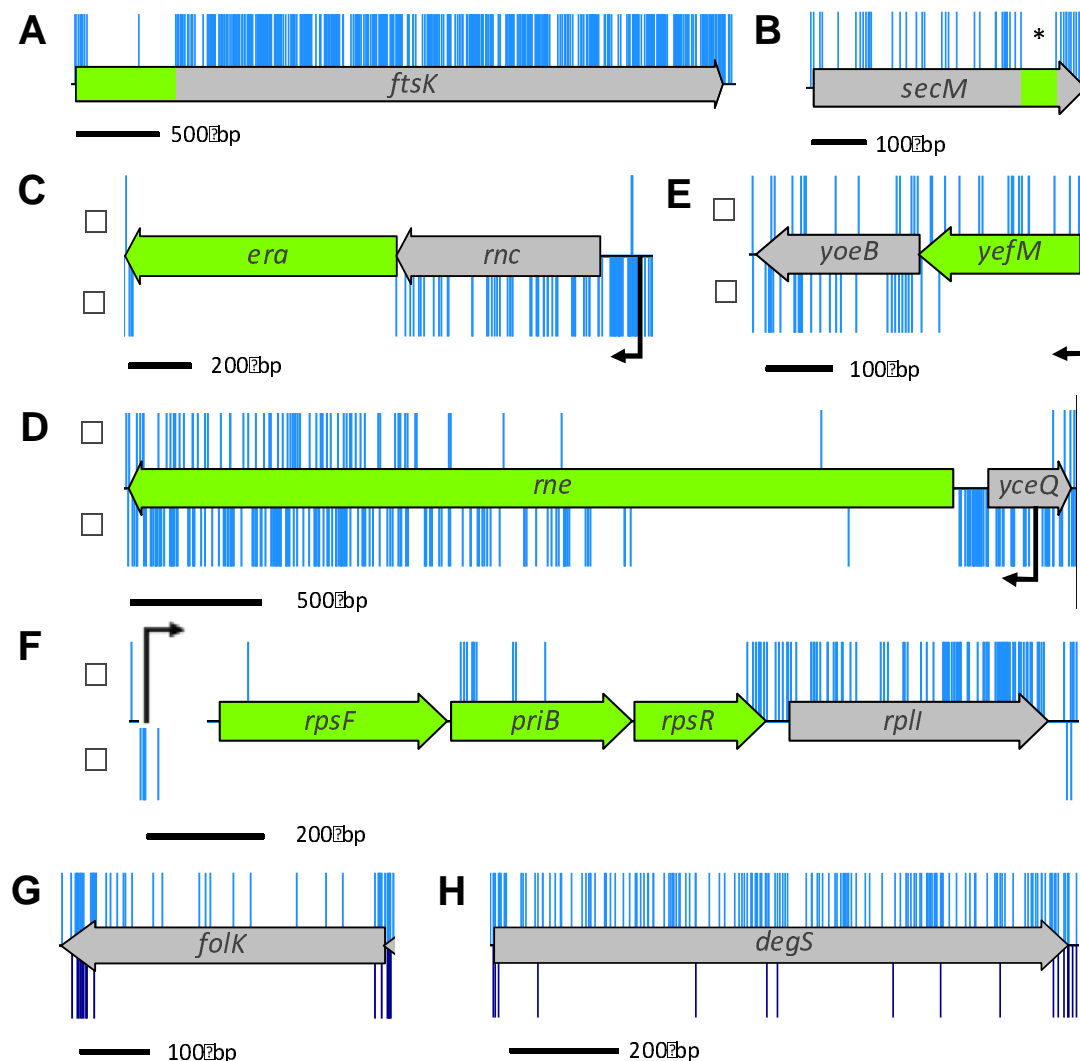


**Figure 3. Insertion profiles of discrepant genes between datasets.** (A) The *ftsK* gene codes for an essential protein in which only part of the protein is required for its essential function. Such genes have a high insertion index score and consequently would not have been identified by automated statistical analysis. (B) *secM* contains a window (\*) of 66 bp in which there were no transposon insertions. This feature is discussed in the text. (C-F) Genes with transposon insertions in only one orientation. The  $\alpha$ - and  $\beta$ -orientation of the transposon is depicted above and below the CDS track respectively, native promoters are shown in black. (G and H) Many transposon insertions were found along the full length of

856 *folK* and *degS* (shown in blue in the upper track of the figure). However, most of these  
857 insertion mutants were lost during outgrowth (lower track below, dark blue).

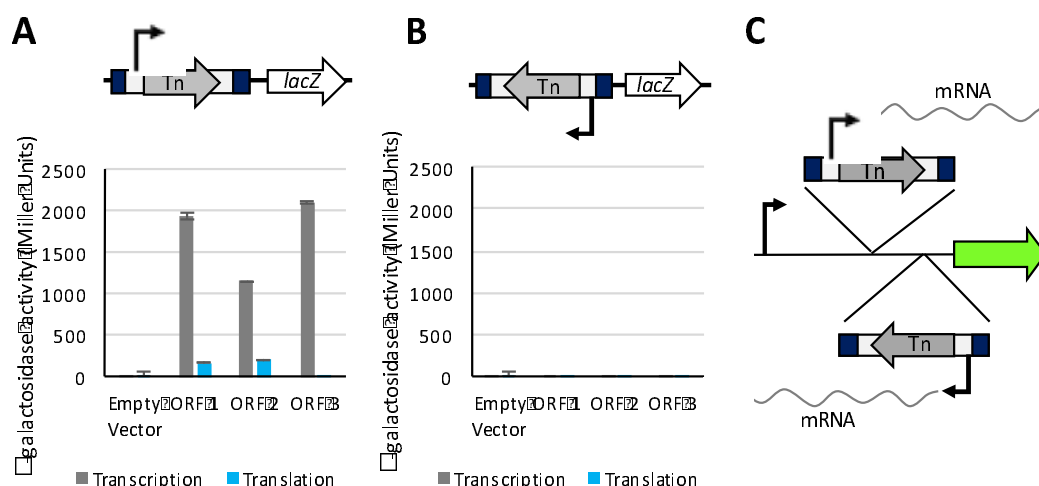


**Figure 4. Transcription and Translation initiation from within the transposon.** The full length mini-Tn5 transposon was cloned into expression vectors pRW224 and pRW225 upstream of the *lacZ* gene, in each orientation, for all three open reading frames (ORF). Vector pRW224 retains a RBS for *lacZ* but no promoter, vector pRW225 has no promoter or RBS upstream of *lacZ*. Vectors pRW224 and pRW225 can be used to detect transcriptional and translational activity respectively. β-galactosidase activity was measured in triplicate for 3 technical replicates, the mean value was plotted with error bars showing the standard deviation between replicates. (A) Transcriptional read-through was confirmed for one orientation of the transposon, consistent with the orientation of the chloramphenicol gene. Translational read-through from the mini-Tn5 transposon was confirmed for 2 out of 3 open reading frames, consistent with GUG (ORF1) and AUG (ORF2) start codons in the transposon inverted repeat. (B) No transcriptional or translational read-through was detected for the opposite orientation of the transposon. (C) Schematic representing the orientation of transposon insertions. The α-orientation of the transposon (upper track) corresponds with the chloramphenicol cassette oriented left to right. The β-orientation (lower track) corresponds with transposon insertions in the opposite direction.

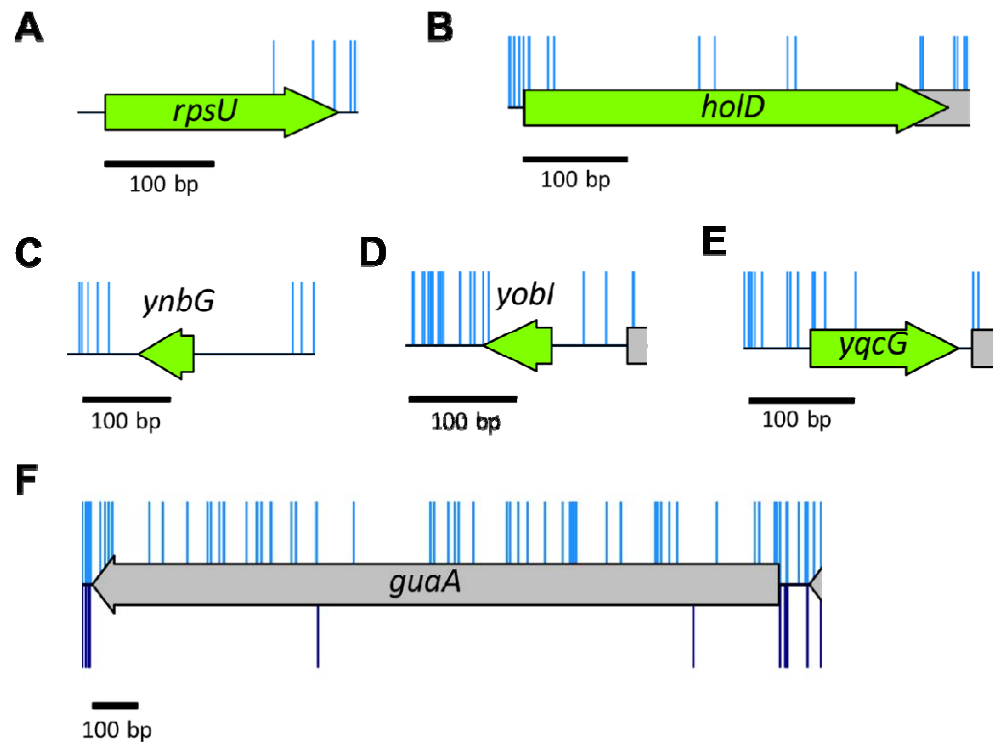


**Figure 5. Essential genes unique to our data.** (A-E) There are very few or no insertions within these genes in our input library (blue). (A & B) Low insertion frequency and literature support classification of these genes as essential. (C, D & E) Recently annotated genes with few or no insertions. Our data suggest these are potentially essential or important for growth. (F) The gene *guaA* has a sufficiently low insertion index score to be classified as essential after initial statistical analysis (blue, above). Following outgrowth, there are few *guaA* mutants (dark blue, below), consistent with literature reports that *guaA* mutants have a growth defect.

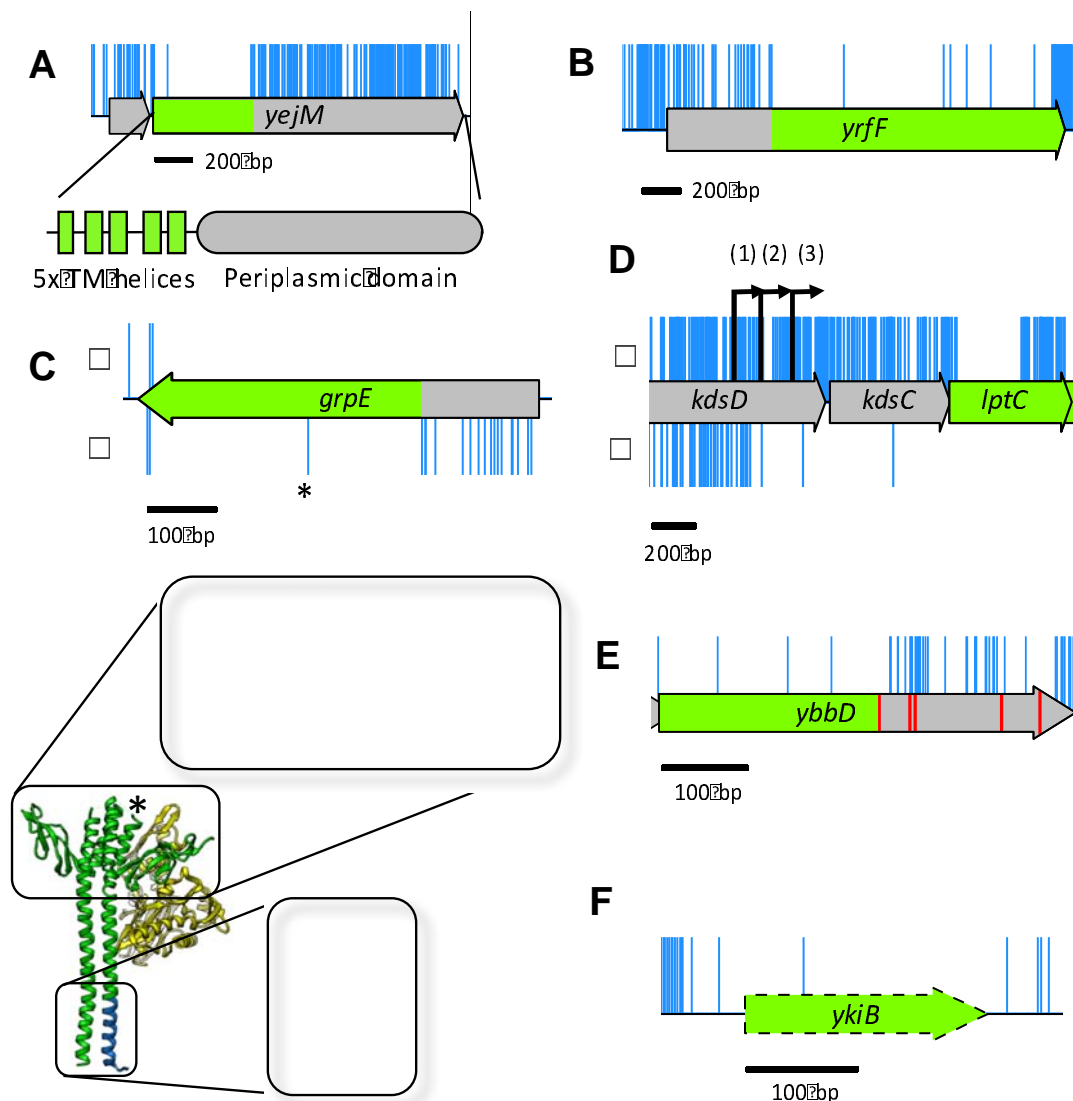
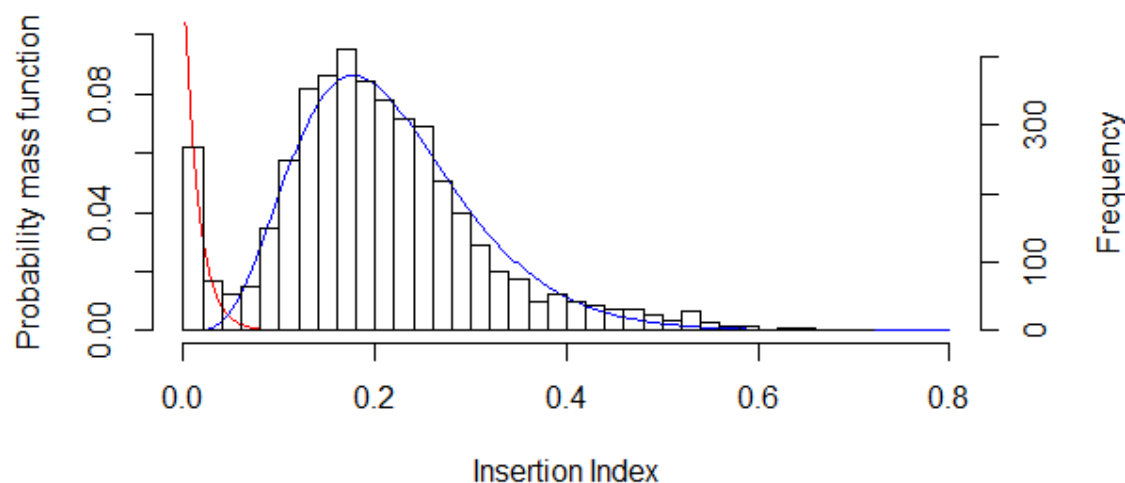


**Figure 6. Additional features identified through detailed analysis of high-resolution insertion data.** (A) Insertions within the CDS but not along the full length correspond with a non-essential periplasmic domain. The 5' end of the CDS has no insertions and corresponds with 5 essential transmembrane domains of YejM. (B) Insertions within *yrfF* suggest a dispensable 5' domain. (C) The *grpE* gene tolerates transposon insertions in the 5' end of the CDS (blue), but only in the orientation that maintains expression of the downstream protein (lower track,  $\beta$ -orientation). The GrpE protein forms a dimer (green) which interacts with DnaK (yellow). Transposon insertions in specific regions of the protein do not disrupt GrpE

893 interaction with DnaK (blue). An additional, single, insertion point in the center of the *grpE*  
894 CDS (\*) maps back to a turn between 2 helices of the GrpE protein. The data reveal  
895 dispensable sections of the GrpE protein and boundaries in secondary structure. (D)  
896 Insertions immediately upstream of *lptC* have an insertion orientation bias. Only insertions  
897 that maintain expression of *lptC* are tolerated within *kdsC* ( $\alpha$ -orientation). The gene *lptC* has  
898 3 promoters ('1', '2' and '3'), the insertion boundary indicate that promoter '2' is the essential  
899 promoter. (E) Pseudogene *ybbD* contains many more insertions after the first stop codon  
900 (red), suggestive that the truncated CDS may still be functional and essential. (F) The  
901 pseudogene *ykiB* is not annotated in the BW25113 genome (CP009273.1) and has a single  
902 insertion within the CDS.  
903

# Supplementary Figures

A



B

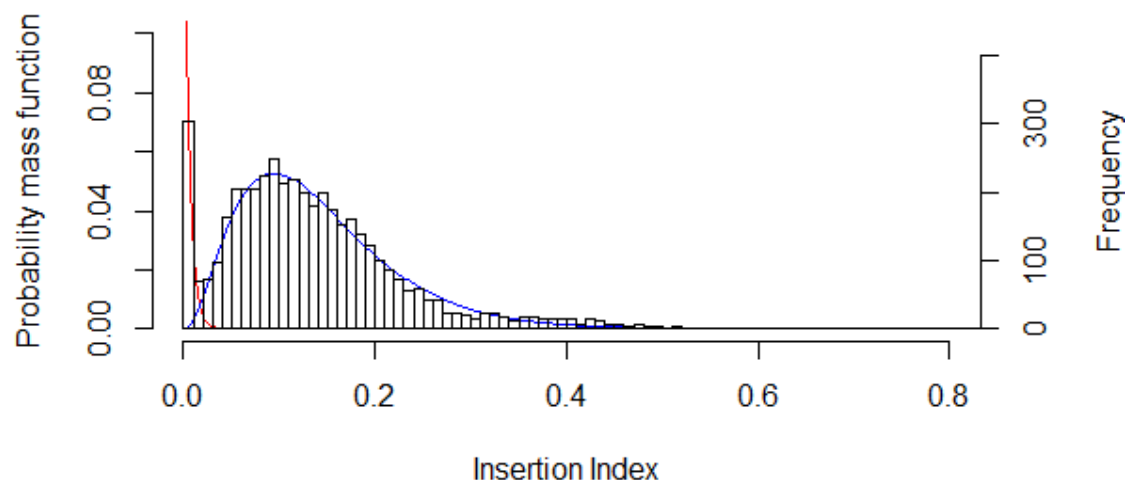


**Figure S1. Frequency distribution of insertion index scores.** The insertion index score for each coding sequence was calculated as the number of insertions per CDS divided by the CDS length in bp to normalize for gene length. The frequency of insertion index scores was plotted for both NTL (A) and LB data (B) and both followed a bimodal distribution. An exponential distribution model was fitted to the left mode that includes essential genes (red) and a gamma distribution model was fitted to the right, non-essential mode (blue). For a

913 given insertion index score, the probability of belonging to each mode was calculated and the  
914 ratio of these values termed the log-likelihood score. A gene was classified as essential if its  
915 log-likelihood score was less than  $\log_2(12)$  and was therefore 12 times more likely to belong  
916 to the red mode than the blue mode

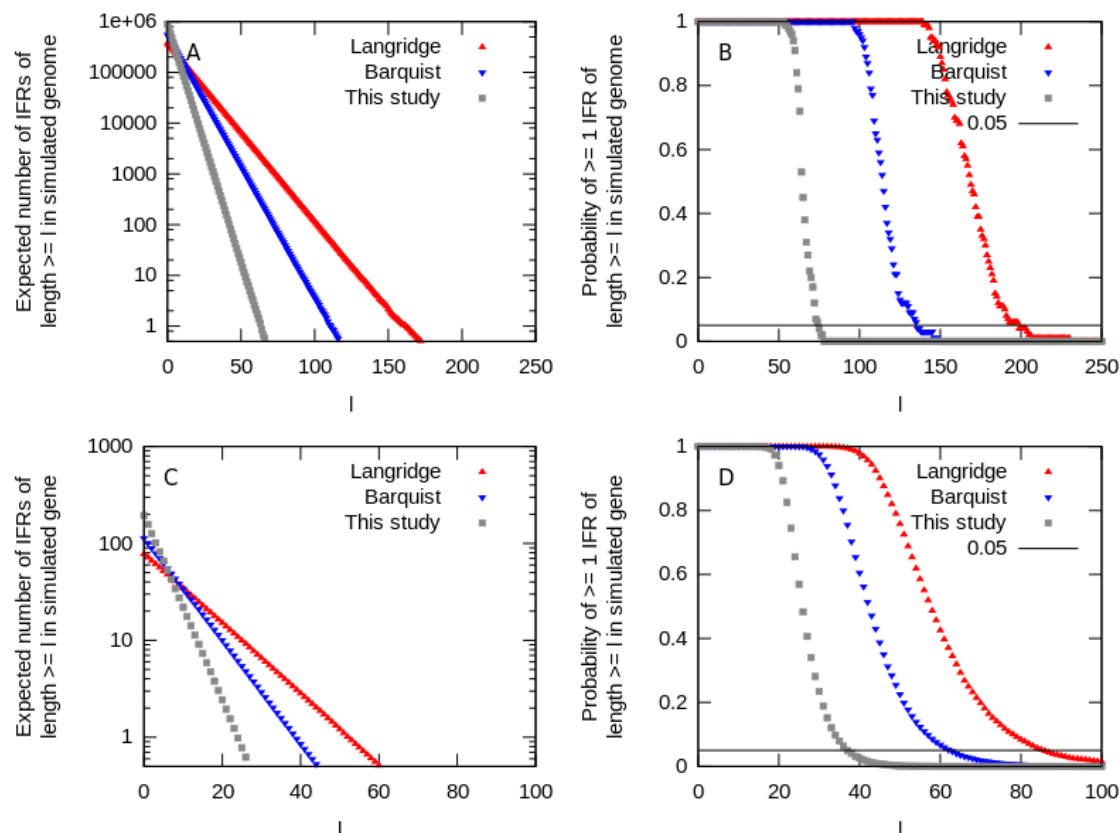


**Figure S2. Simulation of random insertion events for rigorous statistics under the null model of random insertion.** Simulation of random insertion events for rigorous statistics under the null model of random insertion. (A) The expected number of insertion-free regions (IFRs) of length  $l$  or above found in a genome of length  $G$  under the null model of  $N$  random non-coincident insertions.  $G$  and  $N$  are taken to correspond to the statistics in the studies plotted. This expectation is taken over 100 instances of the null model simulation. (B) The (related) probability of at least one IFR of length  $l$  or above occurring anywhere in the simulated genome. (C, D) The same calculation over a simulated gene of length  $g = 1000$ , using  $10^5$  simulation instances.

927 **Supplementary tables.**

928

929 **Table S1. Essential genes identified by TraDIS as essential**

930

931 **Table S2. Comparison of essential genes between datasets**

932

933 **Table S3. Source of discrepancy between datasets**

934 The outlying genes of the venn diagram excluding those unique to our TraDIS data. Gene  
935 names used by the Keio collection are shown in brackets. Venn subcategory is indicated in  
936 column 2 (K = Keio only; KP = Keio and PEC; KT = Keio and TraDIS (this study); P = PEC  
937 only; PT = PEC and TraDIS).

938

939 **Table S4. Essential genes identified by TraDIS analysis after outgrowth in LB.**

940

941 **Supplementary Methods**

942

943 **Statistical Analysis**

944 A Poissonian model, parameterized only by insertion density, gives the probability that no  
945 insertions will be found in a single region of a given length (for example, 60 bases), whereas  
946 genes and genomes have many such regions that are effectively independent. Briefly, if a p-  
947 value of 0.05 is associated with an IFR of length 60 under a simple Poisson model, every  
948 length-60 region in the gene or genome of interest has around a 5% chance of being  
949 insertion-free by chance under the null hypothesis. As a genome will contain many thousand  
950 such regions, many IFRs of length 60 will be expected by chance under the null hypothesis.

A simulation of random insertion events reveals ~2900 IFRs of length 60 or above by random chance in a 4.8Mb genome with 370, 000 insertions (red markers in Fig. S1A).

To correct for this, we need to carefully state the statistic of interest and the corresponding null model. At least three probabilities are pertinent here: those with which, under a null model of random, independent insertions, (i) a single length- $l$  region has no insertions; (ii) a gene of length  $g$  contains one or more IFRs of length  $l$ ; (iii) a genome of length  $G$  contains one or more IFRs of length  $l$ . Previous models have implicitly estimated only (i), but to control the false discovery rate for individual genes or on a genome-wide basis, (ii) and (iii) respectively, are required. An analytic calculation of the corrected p-values corresponding to (ii) and (iii), which we label  $p_{\text{gene}}$  and  $p_{\text{genome}}$ , is laborious; for simplicity and illustrative power we computationally investigate these statistics, simulating many instances of  $N$  random non-coincident insertions in a genome of length  $G$  and reporting the statistics of resultant IFRs (C code available as SI). Reinterpreting the statistics in previous papers on this topic, and assuming a representative gene length of  $g = 1000$ , we find (Fig. S1) that in Langridge *et al.* (371,775 inserts, 4,791,961 base genome), the null model of genome-wide random insertion gives an expected ~16,000 IFRs with  $l \geq 39$  (classified in the original study using the Poisson model as  $p < 0.05$ ) and ~2,900 IFRs with  $l \geq 60$  (classified as  $p < 0.01$ ); the corrected lengths for  $p_{\text{genome}} = 0.05$  and  $p_{\text{gene}} = 0.05$  are ~200 and ~85 respectively (Figures S1B,D; [1]). In Barquist *et al.* (549,086 inserts, 4,878,012 base genome), the null model of genome-wide random insertion gives an expected ~22,000 IFRs of  $l \geq 27$  (classified as  $p < 0.05$ ) and ~4,100 IFRs of  $l \geq 41$  (classified as  $p < 0.01$ ); the corrected lengths for  $p_{\text{genome}} = 0.05$  and  $p_{\text{gene}} = 0.05$  are ~135 and ~62 respectively [2]. Our study (901,383 inserts, 4,631,469 base genome) gives a corrected  $p_{\text{genome}} = 0.05$  of ~75 (and  $p_{\text{gene}} = 0.05$  of ~36).

976

977 A further complication arises because the probability of observing an IFR of given length in a  
 978 gene and the labelling of that gene as essential are not trivially related. Rather, genes are  
 979 classified as essential if their insertion score clusters in the low-score category. While the  
 980 analysis above can therefore give an indication of the resolution of our experiment, further  
 981 theory, perhaps grounded in Hidden Markov Model analysis [3], will be required to forge a  
 982 rigorous connection between the statistics of IFRs and the statistical power associated with  
 983 classification of genes.

984

- 985 [1] Langridge GC, Phan MD, Turner DJ, Perkins TT, Parts L, Haase J, Charles I, Maskell DJ,  
 986 Peters SE, Dougan G, Wain J, Parkhill J, Turner AK. 2009. *Genome Res* 19:2308–2316.
- 987 [2] Barquist L, Langridge G, Turner D, Phan M, Turner AK, Bateman A, Parkhill J, Wain J,  
 988 Gardner P. 2013. *Nucleic Acids Res* 41:4549–4564.
- 989 [3] DeJesus MA, Iorger TR. 2013. *BMC Bioinformatics* 14:303.